DOI: 10.1002/ejic.200900233

Heteroleptic Amidinate Complexes of Heavy Group 15 Elements – Synthesis, X-ray Crystal Structures and Theoretical Calculations

Benjamin Lyhs,[a] Stephan Schulz,*[a] Ulrich Westphal,[a] Dieter Bläser,[a] Roland Boese,[a] and Michael Bolte[b]

Dedicated to Prof. Dietmar Seyferth on the occasion of his 80th birthday

Keywords: N ligands / Main group elements / Antimony / Bismuth

Monosubstituted amidinate complexes $[RC(NR')_2]ECl_2$ [E = Sb, R = *t*Bu, R′ = *i*Pr **1**, Cy **2**, 2,6-$iPr_2C_6H_3$ (Dipp) **3**; R = *n*Bu, R′ = *i*Pr **4**; E = Bi, R = *t*Bu, R′ = *i*Pr **5**, Dipp **6**] were prepared in high yields by salt elimination reactions of ECl_3 with Li amidinates. **1**–**6** were characterized by elemental analyses, NMR and IR spectroscopy and single-crystal X-ray diffraction. In addition, computational calculations were performed to clarify the different bonding modes in **1** and **5**.

Introduction

N,*N*′-Chelating organic ligands L such as β-diketiminate **I**,[1] guanidinate **II**[2] and amidinate anions **III**[3] (Scheme 1) have attracted growing interest in organometallic chemistry in the last decade due to their capability to coordinate very flexible to the metal center as monodentate (η^1, **a**), chelating (η^2, **b**) or bridging monodentate (μ-η^1-η^1, **c**) four-electron donor (Scheme 2).[4] Moreover, they were found very useful in catalysis, material sciences (i.e. precursors for CVD) and organic-inorganic hybrids since their steric and electronic properties can easily be tuned by modification of the organic substituents R and R′.

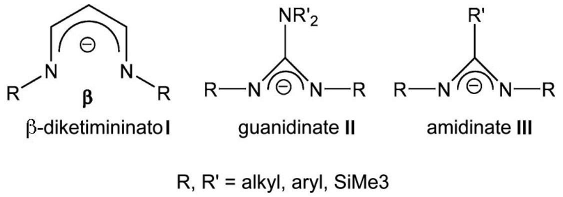

Scheme 1. Typical *N*,*N*′-chelating ligands.

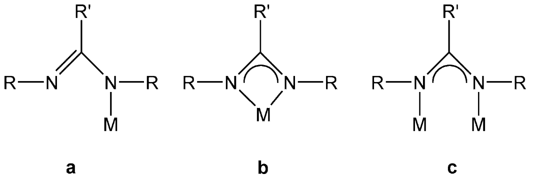

Scheme 2. General coordination modes of amidinate ligands.

In main group element chemistry, research has mainly focused on the synthesis of group 13 element complexes. In particular monosubstituted complexes of the type LMX_2 (M = Al, Ga, In, X = halide, Me) were found to be suitable starting reagents in olefin polymerization reactions and for the synthesis of low-valent group 13 metal complexes of the type LM (M = Al, Ga, In),[5] in which the metal atom formally adopts the oxidation state +I. The same was found for group 2 (Mg) and group 14 metal complexes, in particular LGeX, which were found to be valuable precursors for the synthesis of the corresponding low-valent organomagnesium complexes of the type LMg-MgL {L = ArNC-(N*i*Pr$_2$)NAr (Priso), $[DippNC(Me)]_2CH$ (Dippnacnac)}[6] as well as Ge^I complexes.[7]

Due to our long-term interest in organobismuth and organoantimony chemistry,[8] we became interested in the synthesis of complexes of the type $LECl_2$ (E = Sb, Bi) containing *N*,*N*′-chelating substituents. To our surprise, only a very few group 15 element complexes of types **I**–**III** have been reported in the literature, in particular those of the heaviest elements, Sb and Bi.[9] Only very recently, a very few amidinate,[10] formamidinate[11] and β-diketiminate[12] complexes have been structurally characterized. Moreover, reduction reaction in a very few cases also yielded low-valent amidodiarsene[10] and an unusual β-diiminato arsenic complex.[13]

In an attempt to synthesize potential starting reagents for further reactivity studies, we started to investigate salt elimination reaction between ECl_3 (E = Sb, Bi) and Li ami-

---

[a] Institute of Inorganic Chemistry, University of Duisburg-Essen, 45117 Essen, Germany
Fax: +49-201-1833830
E-mail: stephan.schulz@uni-due.de
[b] Institute of Inorganic Chemistry, University of Frankfurt, 60438 Frankfurt, Germany

Supporting information for this article is available on the WWW under http://www.eurjic.org or from the author.

dinates. Herein, we report on the synthesis of six Sb and Bi amidinate complexes of the general type $LECl_2$ and their X-ray crystal structures.

Results and Discussion

Reactions of equimolar amounts of ECl_3 (E = Sb, Bi) and $Li[RC(NR')_2]$ (R = *n*Bu, *t*Bu; R′ = *i*Pr, Cy, Dipp) in Et_2O yielded the corresponding monosubstituted amidinate complexes of the general type $[tBuC(NR')_2]SbCl_2$ (R′ = *i*Pr **1**, Cy **2**, Dipp **3**), $[nBuC(NiPr)_2]SbCl_2$ (**4**), and $[tBuC(NR')_2]BiCl_2$ (R′ = *i*Pr **5**, Dipp **6**), respectively (Scheme 3). Complexes **1**–**6** were isolated after standard workup in high yields.

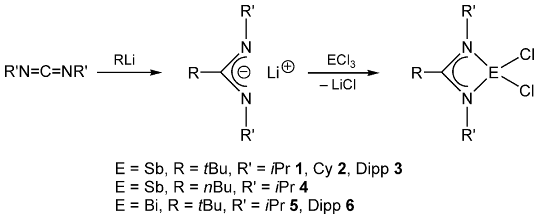

Scheme 3. Synthesis of monosubstituted amidinate complexes **1**–**6**.

^1H and ^{13}C NMR spectra of **1**–**6** show the expected resonances due to the organic substituents (R, R′) of the amidinate moiety. The formation of solvent-coordinated (Et_2O) complexes as was previously observed for comparable bismuth formamidinates of the type $LBiX_2$ (X = Cl, Br) can be excluded for **1**–**6**.[11] Single crystals were obtained from solutions in $CHCl_3$ (**1**–**5**) and THF (**6**) after storage at –30 °C for 48 h (Figures 1, 2, 3, and 4).

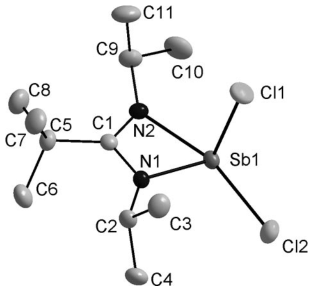

Figure 1. Molecular structure and atom numbering scheme of a monomeric unit of $[tBuC(NiPr)_2]SbCl_2$ (**1**); displacement ellipsoids are drawn at the 50% probability level. Hydrogen atoms have been omitted for clarity.

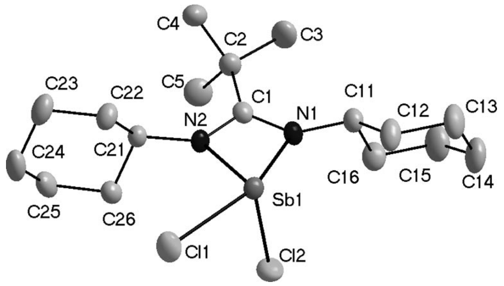

Figure 2. Molecular structure and atom numbering scheme of a monomeric unit of $[tBuC(NCy)_2]SbCl_2$ (**2**); displacement ellipsoids are drawn at the 50% probability level. Hydrogen atoms have been omitted for clarity.

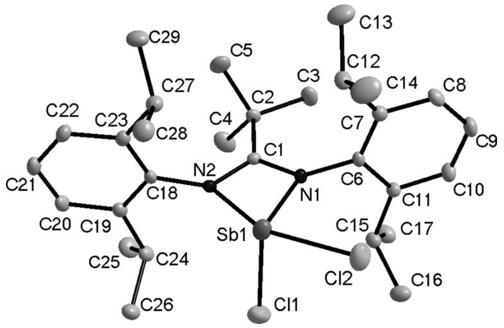

Figure 3. Molecular structure and atom numbering scheme of $[tBuC(NDipp)_2]SbCl_2$ (**3**); displacement ellipsoids are drawn at the 50% probability level. Hydrogen atoms and $CHCl_3$ molecules have been omitted for clarity.

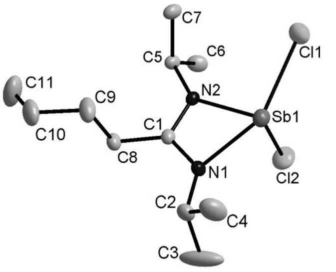

Figure 4. Molecular structure and atom numbering scheme of $[nBuC(NiPr)_2]SbCl_2$ (**4**); displacement ellipsoids are drawn at the 50% probability level. Hydrogen atoms and $CHCl_3$ molecules have been omitted for clarity.

The complexes crystallize in the monoclinic space groups $P2_1/c$ (**1**) and $P2_1/n$ (**2**, **6**), in the orthorhombic space group $Pna2_1$ (**3**) and in the triclinic space group $P\bar{1}$ (**4**, **5**). **3**, **4**, and **5** contain $CHCl_3$ molecules in the crystal lattice whereas **1** and **2** were obtained as solvent-free complexes. In contrast, the Bi center in **6** is weakly coordinated by a THF donor and the crystal lattice contains two additional THF molecules. The amidinate moieties in **1**–**6** serve as chelating (η^2) four-electron donor ligands. The N1–Sb1–N2 [60.69(6)° **1**; 60.41(6)° **2**; 59.21(8)° **3**; 60.99(10)° **4**] and N1–Bi1–N2 bite angles [58.43(18)° **5**] are close to 60° as is typical for metal amidinate complexes whereas that of **6** shows a larger deviation [55.69(11)° **6**]. The N1–C1–N2 angles of **1**–**6** are almost identical and the sum of bond angles at C1 (360.0 **1**, **2**, **3**, **4**, **6**; 359.8 **5**), N1 (360.0 **1**; 359.6 **2**, **3**; 356.8 **4**; 359.9 **5**; 358.3 **6**) and N2 (359.2 **1**; 360.0 **2**; 355.4 **3**; 359.9 **4**, 359.1 **5**, 359.5 **6**) indicate sp^2-hybridized carbon and nitrogen atoms. However, the delocalization of the π-electrons in the amidinate backbone of **1**, **2**, **3**, **4** and **6** is distorted as expressed by the different C1–N1/2 bond lengths. Comparable findings were previously observed in amidinate and guanidinate complexes of the type $LECl_2$ (E = As, Sb).[10,9a] In contrast, **5** shows identical C–N bond lengths, indicating almost perfectly delocalized π-electrons as was reported for $[PhC(NMe)_2ECl_4$ (E = As, Sb)[14] and $[PhC(NMe)_2Sb(Ph)_2$-

Cl_2.[15] In addition, the E1–N1 and E1–N2 bond lengths of **1**–**4** and **6** differ significantly, whereas in **5** almost identical Bi–N bond lengths were observed. Moreover, the most striking structural difference between **1**–**4** and **6** on one hand and **5** on the other hand is reflected by the exocyclic Cl1–E1–Cl2 bond angles, which are significantly smaller in **1**–**4** and **6** compared to the almost linear orientation (Cl1–Bi1–Cl2 [175.02(5)°] as observed in **5** (Figures 5 and 6).

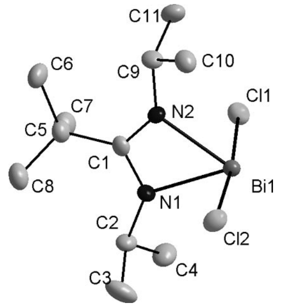

Figure 5. Molecular structure and atom numbering scheme of a monomeric unit of $[tBuC(NiPr)_2]BiCl_2$ (**5**); displacement ellipsoids are drawn at the 50% probability level. Hydrogen atoms and $CHCl_3$ molecules have been omitted for clarity.

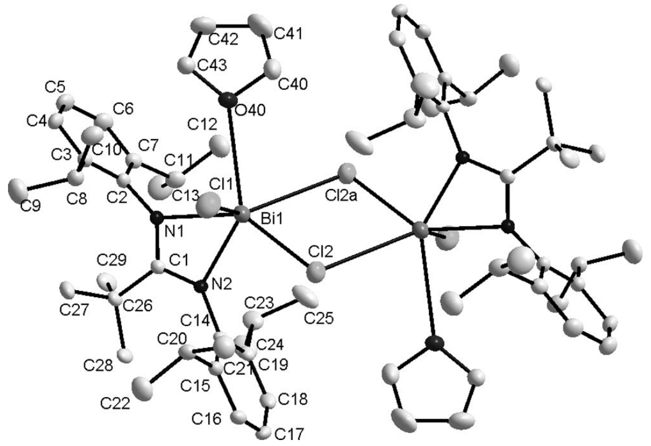

Figure 6. Molecular structure and atom numbering scheme of the dimer of $[tBuC(NDipp)_2]BiCl_2$ (**6**); displacement ellipsoids are drawn at the 50% probability level. Hydrogen atoms and additional THF molecules have been omitted for clarity.

The coordination geometry observed for **1**–**4** can either be described as strongly distorted "saw-horse" or as distorted trigonal bipyramidal conformation with the stereochemically active *electron lone pair* at the Sb atom adopting an equatorial position as was previously observed for group 15 formamidinate complexes.[11] As a consequence, the axial $Sb–Cl_{ax}$ [2.6435(6) **1**; 2.6114(6) **2**; 2.4732(7) **3**; 2.6735(9) Å **4**] and $Sb–N_{ax}$ bond lengths [2.1906(16) **1**; 2.2204(17) **2**; 2.3059(19) **3**; 2.205(3) Å **4**] are significantly elongated compared to the equatorial $Sb–Cl_{Equation}$ [(2).4030(6) **1**; 2.3982(6) **2**; 2.3664(8) **3**; 2.4127(9) Å **4**] and $Sb–N_{eq}$ distances [2.1011(16) **1**, 2.1022(16) **2**; 2.104(2) **3**; 2.116(2) Å **4**]. The $Cl_{ax}–Sb1–N_{ax}$ axes [152.46(5)° **1**; 153.58(5)° **2**; 147.81(6)° **3**; 152.19(8)° **4**] significantly deviate from linearity due to the larger steric demand of the *electron lone pair*.

In remarkable contrast to **3**, which is a monomeric complex in the solid state, solvent-free complexes **1** and **2** as well as **4**, which contains a $CHCl_3$ molecule in the crystal lattice, show weak intermolecular interactions between the axial Cl atom (Cl2 **1**, Cl1 **2**, Cl1 **4**) and an adjacent Sb′ atom, resulting in the formation of asymmetric Sb–Cl–Sb′ bridges. The Sb′–Cl bond lengths are significantly elongated [3.1171(7) **1**, 3.2447(6) **2**, 3.1195(9) Å **4**] compared to the Sb–Cl bonds [2.6435(6) **1**; 2.6114(6) **2**; 2.6735(9) Å **4**], but far below the sum of the van der Waals radii (4.01 Å) and within the range typically observed for anionic chloridoantimonides $Sb_2Cl_8^{2-}$, $Sb_2Cl_{10}^{4-}$, $Sb_2Cl_{11}^{5-}$, and $Sb_4Cl_{16}^{4-}$ (Figure 7).[16]

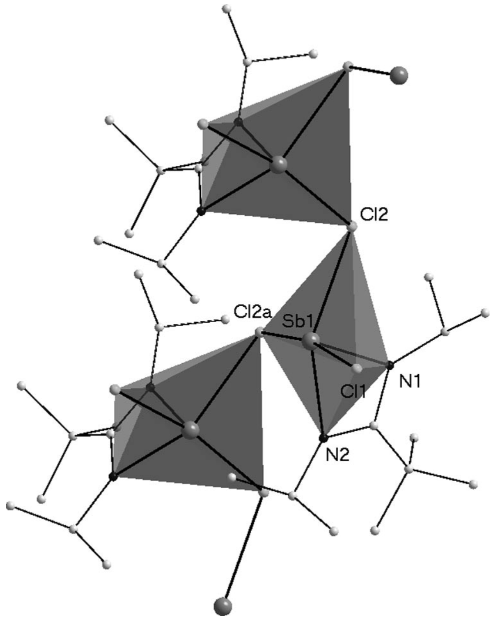

Figure 7. Ball-and-stick/polyhedral presentation of **1**. Hydrogen atoms not shown for clarity.

The Sb′–Cl distances between the second (equatorial) Cl atom and the adjacent Sb′ atom in **1** and **2** are significantly longer (4.7343(7) **1**, 6.5652(6) Å **2**), whereas **4** shows a second weak interaction [3.8972(12) Å]. Consequently, **1** and **2** are best described as corner-bridged oligomers, whereas **4** forms an edge-bridged oligomer. An even more regular structure is observed for **5**, which shows two almost equal intermolecular Cl1/2-Bi′ bond lengths [3.1746(17), 3.2102(19) Å]. Even though these bond lengths are elongated compared to the "regular" Bi–Cl distances [2.7399(18), 2.6868(18) Å], **5** is more symmetric than the dimeric complex $\{[2\text{-}(6\text{-Mepy})NSiMe_3]_2BiCl\}_2$ [Bi′–Cl 2.629(4), 3.554(6) Å].[17b] As a structural consequence, the coordination geometry of Bi atoms in **5** can be described as distorted octahedral (Figure 8).

The distortion most likely results from the small bite angle (N–C–N) of the amidinate moiety, which deviates significantly from the 90° as expected for a regular octahedron. The octahedrons form an edge-shared polymeric structure

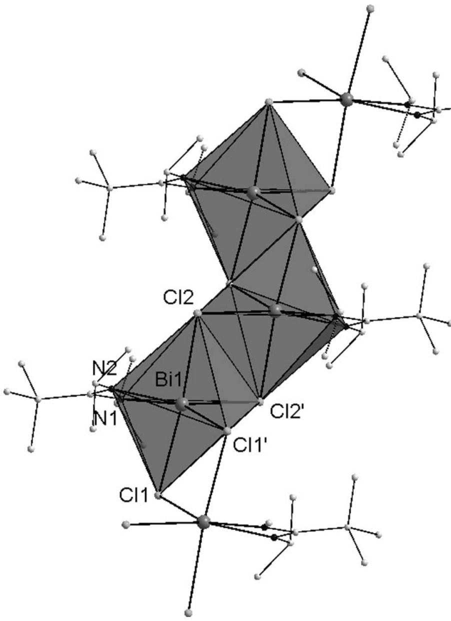

Figure 8. Ball-and-stick/polyhedral presentation of **5**. Hydrogen atoms not shown for clarity.

in the solid state. The *electron lone pair* at the Bi atom is stereochemically inert, which is in remarkable contrast to **1**–**4**. The structure of **5** significantly differs from thf-coordinated, dimeric **6** [Cl-Bi′ 3.4398(10) Å] and from solvent-coordinated monosubstituted formamidinates of the type $LBiCl_2(thf)$ and $[LBiBr_2(thf)]_2$ as recently reported by Jones et al.,[11] which either form centrosymmetric dimers ($[LBiBr_2(thf)]_2$) or adopt a trimeric structure $LBiCl_2(thf)$ with bridging and terminal Cl atoms. The Bi–X–Bi′ bridges (X = Br, Cl) of these formamidinate complexes are asymmetrical and the Bi–X distances range from 2.9–3.1 Å (X = Br) and 2.5–3.7 Å (X = Cl) as was observed for **6**.

The structural parameters as observed for **1**–**6** point to a rather strong influence of both the steric demand of the amidinate ligand as well as the nature of the solvent. **3**, which contains the sterically most demanding amidinate substituent, forms a monomeric structure, whereas **4**, which is sterically slightly less hindered than the analogous *t*Bu-substituted corner-bridged complex **1** forms an edge-bridged oligomeric structure. Coordination of a donor solvent prevents the formation of oligomeric structures as was previously observed for comparable formamidinate complexes.[11]

Theoretical calculations were performed in order to elucidate the different structures of **1** and **5**, in particular their different intermolecular interactions and, as a consequence, their different coordination geometries.[18] Moreover, the electronic nature of the *electron lone pair* was investigated in more detail. Computational calculations starting with the experimental structural data were performed both with the monomeric (**1a**, **5a**) and trimeric units (**1b**, **1c**, **5b**), which represents a small cut of the weakly associated oligomeric complexes. The calculated structural parameters of the trimeric complexes **1b** and **5b** agree slightly better with the experimental values as obtained for **1** and **5** than those of the monomeric complexes **1a** and **5a**. In particular the Cl–Bi–Cl bond angle of the trimer **5b** (179°) agrees much better with the experimentally observed bond angle [175.02(5)°]. The Sb–N and Sb–Cl bond lengths are typically slightly overestimated whereas the intermolecular Bi′–Cl bond length in **5b** is slightly shorter than the experimental value as observed in **5**. Surprisingly, the calculated structure of symmetrically bridged **1c**, which was obtained using the experimental data of **5** as starting point for the structure optimization, is energetically favored by 12 kcal/mol (4 kcal/mol/monomeric unit) compared to **1b**. Moreover, the s-character of the *electron lone pair* of the central Sb atom in **1c** (93.2%) is higher than that in **1b** (87%) and in the monomeric complex **1a** (87.5%). However, these values are still below those calculated for the Bi complexes (**5a**, 94%; **5b**, 97%). According to these calculations, the *electron lone pair* of the Bi complex is less stereochemically active compared to that of the Sb complex, which agrees very well with the different coordination modes as experimentally observed in the solid-state structures of **1** and **5**.

Conclusions

Six monosubstituted amidinate complexes $[RC(NR')_2]ECl_2$ of the heaviest group 15 metals (Sb, Bi) have been prepared and structurally characterized. The central metal (Sb, Bi) as well as the solvent and the steric demand of the amidinate substituent, which can be adjusted by use of different groups R (*n*Bu, *t*Bu) and R′ (*i*Pr, Cy, Dipp), show a distinguished influence to the coordination geometry of the resulting complexes.

Experimental Section

General Procedures: All manipulations were performed under argon using standard Schlenk techniques or in an inert atmosphere glove box. Solvents were dried with Na/K (Et_2O) and CaH_2 ($CHCl_3$) and degassed prior to use. ^1H and $^{13}C\{^1H\}$ NMR spectra were recorded on a Bruker Avance 500 spectrometer and are referenced to internal $CDCl_3$ (^1H: $\delta = 7.24$; ^{13}C: $\delta = 77.0$ ppm). $SbCl_3$ and $BiCl_3$ were commercially available and used after purification (sublimation). Li amidinates $Li[RC(NR')_2]$ were generally prepared by reaction of a carbodiimide with the corresponding organolithium compound. IR spectra were recorded on a ALPHA-T FT-IR spectrometer equipped with a single reflection ATR sampling module. Melting points were measured in sealed capillaries and were not corrected. Elemental analyses were performed at the Elementaranalyse-Labor of the University of Essen.

General Preparation of $LECl_2$ (L = Amidinate, E = Sb, Bi): Solid $Li[RC(NR')_2]$ (R = *n*Bu, *t*Bu; R′ = *i*Pr, Cy, Dipp) was slowly added within 1 h to a solution of ECl_3 in 50 mL of Et_2O at –78 °C, stirred for 1 h and then warmed to ambient temperature over a period of 6 h. The resulting precipitate was filtered and extracted two times with $CHCl_3$ (40 mL). The solvent was evaporated in vacuo, yielding grey (E = Sb) and yellowish crystalline solids (E = Bi), respectively.

[*t*BuC(N*i*Pr)$_2$]SbCl$_2$ (1): *t*BuC(N*i*Pr)$_2$Li (2.50 g, 13.14 mmol), $SbCl_3$ (3.00 g, 13.14 mmol); yield 3.98 g (10.59 mmol, 81%); m.p. 144 °C.

$C_{11}H_{23}Cl_2N_2Sb$ (375.97 g/mol): found (calcd.): H 6.07 (6.17), C 35.01 (35.14), N 7.32 (7.45). ^{1}H NMR (300 MHz, $CDCl_3$, 25 °C): δ = 1.40 [d, $^3J_{HH}$ = 6.6 Hz, 12 H CH(CH_3)$_2$], 1.45 (s, 9 H, *t*Bu), 4.61 [sept, $^3J_{HH}$ = 6.6 Hz, 2 H, *CH*(CH_3)$_2$] ppm. ^{13}C NMR (75 MHz, $CDCl_3$, 25 °C): δ = 24.1 (CH*Me*$_2$), 29.4 (C*Me*$_3$), 40.8 (*C*Me$_3$), 48.9 (*C*HMe$_2$), 176.6 (*C*N$_2$) ppm. IR: $\tilde{\nu}$ = 3013, 2964, 2931, 2871, 1493, 1474, 1381, 1362, 1311, 1186, 1115, 1052, 1023, 926, 797, 676, 558, 491, 443, 413 cm^{-1}.

Table 1. Crystallographic data for [*t*BuC(NR)$_2$]SbCl$_2$ (R = *i*Pr **1**, Cy **2**, Dipp **3**), [*n*BuC(N*i*Pr)$_2$]SbCl$_2$ (**4**) and [*t*BuC(NR)$_2$]BiCl$_2$ (R = *i*Pr **5**, Dipp **6**).

	1	**2**	**3**
Empirical formula	$C_{11}H_{23}Cl_2N_2Sb$	$C_{17}H_{31}Cl_2N_2Sb$	$C_{29}H_{43}Cl_2N_2Sb\cdot 2CHCl_3$
Molecular mass	375.96	456.09	851.04
Crystal system	monoclinic	monoclinic	orthorhombic
Space group	$P2_1/c$	$P2_1/n$	$Pna2_1$
a [Å]	8.9840(2)	12.2083(5)	27.852(5)
b [Å]	21.4667(6)	8.4120(5)	15.962(3)
c [Å]	8.6151(2)	19.7778(8)	8.6085(15)
α [°]	90	90	90
β [°]	111.8150(10)	99.946(3)	90
γ [°]	90	90	90
V [Å^3]	1542.50(7)	2000.58(17)	3827.1(12)
Z	4	4	4
T [K]	193(2)	173(2)	173(1)
Radiation λ [Å]	0.71073	0.71073	0.71073
μ [mm^{-1}]	2.115	1.646	1.303
$D_{calcd.}$ [g cm^{-3}]	1.619	1.514	1.477
$2\theta_{max}$ [°]	61.0	55.8	58.9
Crystal dimensions [mm]	0.26 × 0.23 × 0.21	0.31 × 0.13 × 0.12	0.36 × 0.18 × 0.16
Number of reflections	39764	34204	75324
Number of unique reflections	4529	4603	10336
R_{merg}	0.0262	0.0708	0.0590
Number of parameters Restraints	146/0	200/0	391/1
$R1$[a]	0.0237	0.0266	0.0309
$wR2$[b]	0.0516	0.0688	0.0714
Goodness of fit[c]	1.335	1.027	0.993
Final max./min. $\Delta\rho$/e·Å^{-3}	0.526/–1.056	0.533/–0.848	0.628/–0.660
	4	**5**	**6**[d]
Empirical formula	$C_{11}H_{23}Cl_2N_2Sb\cdot CHCl_3$	$C_{22}H_{46}Bi_2Cl_4N_4\cdot 4CHCl_3$	$C_{29}H_{43}Cl_2N_2Bi\cdot 3[C_4H_8O]$
Molecular mass	495.33	1403.86	915.85
Crystal system	triclinic	triclinic	monoclinic
Space group	$P\bar{1}$	$P\bar{1}$	$P2_1/n$
a [Å]	8.4646(9)	8.5021(5)	15.0780(3)
b [Å]	10.2032(11)	11.4961(7)	21.7447(5)
c [Å]	13.1082(15)	13.2404(9)	15.4864(3)
α [°]	91.661(6)	102.238(4)	90
β [°]	96.985(6)	104.223(4)	111.3847(12)
γ [°]	113.195(5)	98.007(3)	90
V [Å^3]	1029.2(2)	1200.68(13)	4727.90(17)
Z	2	1	4
T [K]	173(2)	173(1)	173(1)
Radiation λ [Å]	0.71073	0.71073	0.71073
μ [mm^{-1}]	1.983	8.233	3.875
$D_{calcd.}$ [g cm^{-3}]	1.598	1.942	1.287
$2\theta_{max}$ [°]	57.1	52.8	55.0
Crystal dimensions [mm]	0.34 × 0.25 × 0.18	0.17 × 0.13 × 0.07	0.27 × 0.22 × 0.13
Number of reflections	20366	24247	72955
Number of unique reflections	5042	5935	13170
R_{merg}	0.0351	0.0658	0.0670
Number of parameters Restraints	209/0	218/0	514/0
$R1$[a]	0.0399	0.0447	0.0370
$wR2$[b]	0.893	0.1138	0.1012
Goodness of fit[c]	1.037	1.008	1.038
Final max./min. $\Delta\rho$/e·Å^{-3}	1.030/–0.899	3.326/–3.863	2.472/–0.763

[a] $R1 = \Sigma(||F_o| - |F_c||)/\Sigma|F_o|$ [for $I > 2\sigma(I)$]. [b] $wR2 = \{\Sigma[w(F_o^2 - F_c^2)^2]/\Sigma[w(F_o^2)^2]\}^{1/2}$. [c] Goodness of fit = $\{\Sigma[w(|F_o^2|\ |F_c^2|)^2]/(N_{obs.}/N_{param.})\}^{1/2}$. [d] *t*Bu carbon atoms C(27) to C(29) disordered over two sites with SOF 0.5, THF molecules O(60), C(60) to C(63) and O(70), C(70) to C(73) refined with reduced SOF 0.5 together with the riding hydrogen atoms. In spite of the reduced SOFs of the solvent molecules, the ADPs still indicate severe disorder which could not be resolved.

[*t*BuC(NCy)$_2$]SbCl$_2$ (2): *t*BuC(NCy)$_2$Li (2.50 g, 9.25 mmol), SbCl$_3$ (2.11 g, 9.25 mmol); yield 3.29 g (7.22 mmol, 78%); m.p. 205 °C (dec.). $C_{17}H_{31}Cl_2N_2Sb$ (456.10 g/mol): found (calcd.): H 6.72 (6.85), C 44.57 (44.77), N 6.08 (6.14)%. ^{1}H NMR (500 MHz, CDCl$_3$, 25 °C): δ = 1.16–1.87 (m, 20 H, N*Cy*), 1.44 (s, 9 H, *t*Bu), 4.11 (m, 2 H, N*CH*C$_5$H$_{10}$) ppm. ^{13}C NMR (75 MHz, CDCl$_3$, 25 °C): δ = 24.9 (C3/C5); 25.8 (C4), 29.4 (C*Me*$_3$), 34.5 (C2/C6), 41.2 (*C*Me$_3$), 57.2 (N-C1), 177.8 (*C*N$_2$) ppm. IR: $\tilde{\nu}$ = 2962, 2924, 2847, 1595, 1518, 1452, 1425, 1405, 1377, 1341, 1309, 1299, 1259, 1172, 1015, 889, 865, 795, 712, 660, 629, 484 cm^{-1}.

[*t*BuC(NDipp)$_2$]SbCl$_2$ (3): *t*BuC(NDipp)$_2$Li (5.61 g, 13.14 mmol), SbCl$_3$ (3.00 g, 13.14 mmol); yield 5.88 g (9.61 mmol, 73%); m.p. 182 °C. $C_{29}H_{43}Cl_2N_2Sb$ (612.33 g/mol): found (calcd.): H 7.05 (7.08), C 56.87 (56.89), N 4.51 (4.57)%. ^{1}H NMR (300 MHz, CDCl$_3$, 25 °C): δ = 0.98 (s, 9 H, *t*Bu), 1.30 [d, $^3J_{HH}$ = 6.6 Hz, 12 H, CH(*CH*$_3$)$_2$], 1.34 [d, $^3J_{HH}$ = 6.9 Hz, 12 H, CH(*CH*$_3$)$_2$], 3.30 [m, 4 H, *CH*(CH$_3$)$_2$], 7.18 (m, 6 H, Ar*H*) ppm. ^{13}C NMR (75 MHz, CDCl$_3$, 25 °C): δ = 23.0 (CH*Me*$_2$), 26.9 (*C*HMe$_2$), 29.1 (C*Me*$_3$), 41.9 (*C*Me$_3$), 123.6 (C4), 127.0 (C3/C5), 136.6 (C2/C6), 144.9 (N-C1), 174.8 (*C*N$_2$) ppm. IR: $\tilde{\nu}$ = 2962, 2929, 2868, 1522, 1437, 1382, 1362, 1315, 1254, 1228, 1175, 1094, 1007, 798, 784, 761, 714, 663, 435, 401 cm^{-1}.

[*n*BuC(N*i*Pr)$_2$]SbCl$_2$ (4): *n*BuC(N*i*Pr)$_2$Li (2.50 g, 13.14 mmol), SbCl$_3$ (3.00 g, 13.14 mmol); yield 4.10 g (10.91 mmol, 83%); m.p. 82 °C. $C_{11}H_{23}Cl_2N_2Sb$ (375.97 g/mol): found (calcd.): H 6.12 (6.17), C 35.10 (35.14), N 7.34 (7.45)%. ^{1}H NMR (300 MHz, CDCl$_3$, 25 °C): δ = 0.95 (t, $^3J_{HH}$ = 7.2 Hz, 3 H, CH$_2$CH$_2$CH$_2$*CH*$_3$), 1.30 [d, $^3J_{HH}$ = 6.6 Hz, 12 H, CH(*CH*$_3$)$_2$], 1.42 (m, 2 H, CH$_2$CH$_2$*CH*$_2$CH$_3$), 1.53 (m, 2 H, CH$_2$*CH*$_2$CH$_2$CH$_3$), 2.30 (m, 2 H, *CH*$_2$CH$_2$CH$_2$CH$_3$), 4.04 [sept, $^3J_{HH}$ = 6.6 Hz, 2 H, *CH*(CH$_3$)$_2$] ppm. ^{13}C NMR (75 MHz, CDCl$_3$, 25 °C): δ = 13.7 (CH$_2$-CH$_2$-CH$_2$-*CH*$_3$), 22.9 (CH$_2$-CH$_2$-*CH*$_2$-CH$_3$), 24.1 (CH*Me*$_2$), 27.1 (CH$_2$-*CH*$_2$-CH$_2$-CH$_3$), 29.0 (*CH*$_2$-CH$_2$-CH$_2$-CH$_3$), 47.8 (*C*HMe$_2$), 172.6 (*C*N$_2$) ppm. IR: $\tilde{\nu}$ = 2964, 2929, 2870, 1643, 1522, 1464, 1451, 1436, 1363, 1336, 1258, 1227, 1203, 1028, 1078, 949, 839, 796, 687, 614, 564, 454, 414 cm^{-1}.

[*t*BuC(N*i*Pr)$_2$]BiCl$_2$ (5): *t*BuC(N*i*Pr)$_2$Li (2.50 g, 13.14 mmol), BiCl$_3$ (4.15 g, 13.14 mmol); yield 4.57 g (9.86 mmol, 75%); m.p. 170 °C (dec.). $C_{11}H_{23}BiCl_2N_2$ (463.20 g/mol): found (calcd.): H 5.12 (5.00), C 28.47 (28.52), N 5.80 (6.05)%. ^{1}H NMR (300 MHz, CDCl$_3$, 25 °C): δ = 1.35 [d, $^3J_{HH}$ = 6.2 Hz, 12 H, CH(*CH*$_3$)$_2$], 1.53 (s, 9 H, *t*Bu), 6.77 [sept, $^3J_{HH}$ = 6.2 Hz, 2 H, *CH*(CH$_3$)$_2$] ppm. ^{13}C NMR (75 MHz, CDCl$_3$, 25 °C): δ = 25.9 (CH*Me*$_2$), 29.8 (C*Me*$_3$), 48.2 (*C*Me$_3$), 52.8 (*C*HMe$_2$), 177.8 (*C*N$_2$) ppm. IR: $\tilde{\nu}$ = 2964, 2927, 2880, 1615, 1489, 1452, 1409, 1368, 1311, 1183, 1115, 1046, 925, 803, 671, 553, 474 cm^{-1}.

[*t*BuC(NDipp)$_2$]BiCl$_2$ (6): *t*BuC(NDipp)$_2$Li (5.61 g, 13.14 mmol), BiCl$_3$ (4.15 g, 13.14 mmol); yield 7.25 g (10.36 mmol, 79%); m.p. 183 °C (dec.). $C_{29}H_{43}BiCl_2N_2$ (699.56 g/mol): found (calcd.): H 6.13 (6.19), C 49.53 (49.79), N 3.89 (4.00)%. ^{1}H NMR (300 MHz, CDCl$_3$, 25 °C): δ = 1.07 (s, 9 H, *t*Bu), 1.32 [d, $^3J_{HH}$ = 6.9 Hz, 12 H, CH(*CH*$_3$)$_2$], 1.39 [d, $^3J_{HH}$ = 6.9 Hz, 12 H, CH(*CH*$_3$)$_2$], 3.47 [m, 4 H, *CH*(CH$_3$)$_2$], 7.09 (m, 6 H, Ar*H*) ppm. ^{13}C NMR (75 MHz, CDCl$_3$, 25 °C): δ = 23.2 (CC*Me*$_3$), 27.9 (CH*Me*$_2$), 28.5 (CH*Me*$_2$), 29.7 (*C*HMe$_2$), 49.5 (C*C*Me$_3$), 123.1 (C4), 127.6 (C3/C5), 136.7 (C2/C6), 145.7 (N-C1), 172.8 (*C*CMe$_3$) ppm. IR: $\tilde{\nu}$ = 2959, 2864, 1616, 1433, 1362, 1316, 1258, 1213, 1173, 1091, 1013, 931, 866, 797, 761, 661, 474, 430, 396 cm^{-1}.

Single Crystal X-ray Analysis: Crystallographic data of **1**–**6** are summarized in Table 1 and bond lengths and angles are given in Tables 2 and 3. Figures 1, 2, 3, 4, 5, and 6 show ORTEP diagrams of the solid-state structures of **1**–**6**. Data were collected on a Bruker AXS SMART APEX CCD (**1**, **3**–**6**) and a Stoe IPDS-II (**2**) diffractometer, [Mo-K_α radiation, λ = 0.71073 Å; T = 173(2) K]. The structures were solved by Direct Methods (SHELXS-97)[19] and refined by full-matrix least-squares on F^2 (SHELXL-97, program for crystal structure refinement).[20] Semi-empirical absorption corrections were applied.

CCDC-723192 (for **1**), -723197 (for **2**), -723195 (for **3**), -723194 (for **4**), -723193 (for **5**), -723196 (for **6**) contain the supplementary crystallographic data for this paper. These data can be obtained free of charge from The Cambridge Crystallographic Data Centre via www.ccdc.cam.ac.uk/data_request/cif.

Supporting Information (see also the footnote on the first page of this article): Tables of selected structural parameters, absolute energies and atomic charges of **1a**, **1b**, **1c**, **5a**, and **5b**, which were calculated from NBO population analyses, are given in the supplement.

Table 2. Selected bond lengths [Å] and angles [°] of [*t*BuC(NR)$_2$]SbCl$_2$ (R = *i*Pr **1**, Cy **2**, Dipp **3**) and [*n*BuC(N*i*Pr)$_2$]SbCl$_2$ (**4**) and [*t*BuC(NR)$_2$]BiCl$_2$ (R = *i*Pr **5**, Dipp **6**).

	1	**2**	**3**	**4**	**5**	**6**
E1–N1/	2.1011(16)/	2.2204(17)/	2.104(2)/	2.205(3)/	2.236(5)/	2.408(3)/
E1–N2	2.1906(17)	2.1022(16)	2.3059(19)	2.116(2)	2.243(5)	2.265(3)
E1–Cl1/	2.4030(6)/	2.6114(6)/	2.3664(8)/	2.6735(9)/	2.7399(18)/	2.4640(12)/
E1–Cl2	2.6435(6)	2.3982(6)	2.4732(7)	2.4127(9)	2.6868(18)	2.6171(10)
E1–Cl1/2a	3.1171(7)/	3.2447(6)/	> 8.5	3.1195(9)/	3.1746(17)/	3.4398(10)/
	4.7343(7)	6.5652(6)		3.8972(12)	3.2102(19)	6.4022(12)
C1–N1/	1.352(2)/	1.320(3)/	1.361(3)/	1.319(4)/	1.336(8)/	1.316(5)/
C1–N2	1.320(2)	1.366(3)	1.323(3)	1.346(4)	1.337(8)	1.341(5)
C1–C_R	1.536(3)	1.540(3)	1.543(3)	1.499(5)	1.554(9)	1.561(5)
N1–$C_{R'}$/	1.469(2)/	1.461(3)/	1.437(3)/	1.460(4)/	1.464(7)/	1.422(5)/
N2–$C_{R'}$	1.470(3)	1.469(3)	1.430(3)	1.470(4)	1.466(8)	1.438(5)
N1–E1–N2	60.69(6)	60.41(6)	59.21(8)	60.99(10)	58.43(18)	55.69(11)
N1–C1–N2	108.56(16)	108.29(18)	109.0(2)	110.8(3)	109.8(5)	110.8(3)
Cl1–E1–Cl2	88.02(2)	87.65(2)	90.27(3)	95.49(7)	175.02(5)	89.05(4)
Cl1–E1–N1/	94.90(5)/	153.58(5)/	98.89(6)/	152.19(8)/	84.94(15)/	89.90(9)/
Cl1–E1–N2	88.02(5)	94.53(5)	88.48(6)	91.43(7)	86.46(14)	97.14(9)
Cl2–E1–N1/	92.55(5)/	87.41(5)/	89.29(6)/	92.30(8)/	90.60(15)/	141.99(8)/
Cl2–E1–N2	152.46(5)	97.07(5)	147.81(6)	93.12(7)	89.31(14)	86.78(9)

Table 3. Selected bond lengths [Å] and angles [°] of the calculated structures of [tBuC(NiPr)$_2$]ECl$_2$ (E = Sb **1**, Bi **5**).

	E–N	E–Cl	C–N	Cl–E–Cl	N–E–N
1 (XRD)	2.1011(16)/ 2.1906(17)	2.4030(6)/2.6435(6)/ 3.1171(7)/4.7343(7)	1.352(2)/ 1.320(2)	88.02(2)	60.69(6)
1a (SDD) monomer	2.13/2.28	2.50/2.60	1.34/1.39	91	64
1b (SDD) trimer	2.13/2.23	2.52/2.74/3.41/4.56	1.34/1.38	90	61
1c (SDD) trimer[a]	2.16/2.18	2.76/2.76/3.16/3.21	1.36/1.37	177	61
5 (XRD)	2.236(5)/2.243(5)	2.7399(18)/ 2.6868(18)/ 3.1746(17)/ 3.2102(19)	1.336(8)/1.337(8)	175.02(5)	58.43(18)
5a (SDD) monomer	2.24	2.69	1.36/1.37	165	58
5b (SDD) trimer	2.28/2.30	2.81/2.83/3.03/3.06	1.36/1.37	179	58

[a] Structure optimization using the structural parameter of the Bi complex (monomeric unit).

Acknowledgments

S. S. thanks Deutsche Forschungsgemeinschaft (DFG) for financial support.

---

[1] L. Bourget-Merle, M. F. Lappert, J. R. Severn, *Chem. Rev.* **2002**, *102*, 3031.

[2] P. J. Bailey, S. Pace, *Coord. Chem. Rev.* **2001**, *214*, 91.

[3] a) J. Barker, M. Kilner, *Coord. Chem. Rev.* **1994**, *133*, 219; b) P. C. Junk, M. L. Cole, *Chem. Commun.* **2007**, 1579. For a very recent review on amidinate and guanidinate complexes see: c) F. Edelmann, *Adv. Organomet. Chem.* **2008**, *57*, 183. The coordination chemistry of neutral amidines and guanidines was recently described; d) M. P. Coles, *J. Chem. Soc., Dalton Trans.* **2006**, 985.

[4] See for further bindings modes: P. C. Junk, M. L. Cole, *Chem. Commun.* **2007**, 1579.

[5] a) C. Cui, H. W. Roesky, H.-G. Schmidt, M. Noltemeyer, H. Hao, F. Cimpoesu, *Angew. Chem. Int. Ed.* **2000**, *39*, 4274; b) N. J. Hardman, B. E. Eichler, P. P. Power, *Chem. Commun.* **2000**, 1991; c) C. Jones, P. C. Junk, J. A. Platts, A. Stasch, *J. Am. Chem. Soc.* **2006**, *128*, 2206; d) G. Jin, C. Jones, P. C. Junk, A. Stasch, W. D. Woodul, *New J. Chem.* **2008**, *32*, 835.

[6] S. P. Green, C. Jones, A. Stasch, *Science* **2007**, *318*, 1754.

[7] See the following and references cited therein: a) M. Stender, A. D. Phillips, P. P. Power, *Inorg. Chem.* **2001**, *40*, 5314; b) S. P. Green, C. Jones, P. C. Junk, K.-A. Lippert, A. Stasch, *Chem. Commun.* **2006**, 3978; c) A. Stasch, C. M. Forsyth, C. Jones, P. C. Junk, *New J. Chem.* **2008**, *32*, 829; d) S. Nagendran, S. S. Sen, H. W. Roesky, D. Koley, H. Grubmüller, A. Pal, R. Herbst-Irmer, *Organometallics* **2008**, *27*, 5459.

[8] a) S. Schulz, M. Nieger, *Angew. Chem.* **1999**, *111*, 1020; *Angew. Chem. Int. Ed.* **1999**, *38*, 967; b) A. Kuczkowski, S. Schulz, M. Nieger, *Organometallics* **2001**, *20*, 2000; c) A. Kuczkowski, S. Schulz, M. Nieger, *Angew. Chem.* **2001**, *113*, 4351; *Angew. Chem. Int. Ed.* **2001**, *40*, 4222.

[9] a) C. Ergezinger, F. Weller, K. Dehnicke, *Z. Naturforsch. B Chem. Sci.* **1988**, *43*, 1119; b) U. Patt-Seibel, U. Müller, C. Ergezinger, B. Borgsen, K. Dehnicke, D. Fenske, G. Baum, *Z. Anorg. Allg. Chem.* **1990**, *582*, 30; c) P. J. Bailey, R. O. Gould, C. N. Harmer, S. Pace, A. Steiner, D. S. Wright, *Chem. Commun.* **1997**, 1161; d) C. L. Raston, R. W. Skelton, V.-A. Tolhurst, A. H. White, *Polyhedron* **1998**, *17*, 935; e) C. L. Raston, B. W. Skelton, V. A. Tolhurst, A. H. White, *J. Chem. Soc., Dalton Trans.* **2000**, 1279. Moreover, several boramidinate complexes and complexes with the group 15 element in the formal oxidation state +5 have been structurally characterized; f) J. Konu, M. S. Balakrishna, T. Chivers, T. W. Swaddle, *Inorg. Chem.* **2007**, *46*, 2627; g) F. Weller, J. Pebler, K. Dehnicke, K. Hartke, H.-M. Wolff, *Z. Anorg. Allg. Chem.* **1982**, *486*, 61; h) W. Honeise, W. Schwarz, G. Heckmann, A. Schmidt, *Z. Anorg. Allg. Chem.* **1986**, *533*, 55.

[10] S. P. Green, C. Jones, G. Jin, A. Stasch, *Inorg. Chem.* **2007**, *46*, 8.

[11] M. Brym, C. M. Forsyth, C. Jones, P. C. Junk, R. P. Rose, A. Stasch, D. A. Turner, *Dalton Trans.* **2007**, 3282.

[12] a) L. A. Lesikar, A. F. Richards, *J. Organomet. Chem.* **2006**, *691*, 4250; b) L. W. Pineda, V. Jancik, S. Nembenna, H. W. Roesky, *Z. Anorg. Allg. Chem.* **2007**, *633*, 2205. In addition, complexes containing dianionic diamidonapthole substituents have been prepared:; c) H. A. Spinney, I. Korobkov, G. A. DiLabio, G. P. A. Yap, D. S. Richeson, *Organometallics* **2007**, *26*, 4972; d) H. A. Spinney, I. Korobkov, D. S. Richeson, *Chem. Commun.* **2007**, 1647.

[13] P. B. Hitchcock, M. F. Lappert, G. Li, A. V. Protchenko, *Chem. Commun.* **2009**, 428.

[14] W. Honeise, W. Schwarz, G. Heckmann, A. Schmidt, *Z. Anorg. Allg. Chem.* **1986**, *533*, 55.

[15] F. Weller, J. Pebler, K. Dehnicke, K. Hartke, H.-M. Wolff, *Z. Anorg. Allg. Chem.* **1982**, *486*, 61.

[16] According to a structure search in the *Cambridge Structural Database*, as described anions typically show bridging Sb–Cl bond lengths ranging from 3.00–3.30 Å.

[17] a) C. L. Raston, B. W. Skelton, V.-A. Tolhurst, A. H. White, *J. Chem. Soc., Dalton Trans.* **2000**, 1279; b) C. L. Raston, B. W. Skelton, V.-A. Tolhurst, A. H. White, *Polyhedron* **1998**, *17*, 935.

[18] DFT calculations were carried out with the Gaussian03 suite of programs (M. J. Frisch, et al. *Gaussian 03*, Revision D.02; Gaussian Inc., Pittsburgh, PA, 2003, complete reference is given in the supplement). The molecular structures and energies of compounds **1a**, **1b**, **1c**, **5a**, and **5b** were obtained by performing a complete energy optimization of all geometric parameters at the b3lyp/sdd level (input keywords "# b3lyp/sdd opt pop = nbo′′), using the atomic coordinate of the crystal structure determination of **1** and **5** (without solvent molecule) as starting point. Population analysis was carried out with the NBO module as implemented in Gaussian03. The final molecular structures and list of the final atomic coordinates and energies, selected bond lengths, and NBO atomic populations are given in the electronic supplement.

[19] SHELXS-97, Program for Structure Solution: G. M. Sheldrick, *Acta Crystallogr., Sect. A* **1990**, *46*, 467.

[20] G. M. Sheldrick, *SHELXL-97*, Program for Crystal Structure Refinement, University of Göttingen, Germany, **1997**.

Received: March 12, 2009